Supplementary Information

Effect of Hartree-Fock Pseudopotentials on Local Density Functional Theory Calculations

Hengxin Tan[1], Yuanchang Li[2], Shengbai Zhang[3,4], and Wenhui Duan[1,5]

[1]State Key Laboratory of Low-Dimensional Quantum Physics and Collaborative Innovation Center of Quantum Matter, Department of Physics, Tsinghua University, Beijing 100084, China

[2]Advanced Research Institute of Multidisciplinary Science, Beijing Institute of Technology, Beijing 100081, China

[3]Beijing Computational Science Research Center, No.10 East Xibeiwang Road, Beijing 100193, China

[4]Department of Physics, Applied Physics and Astronomy, Rensselaer Polytechnic Institute, Troy, NY, 12180, USA

[5]Institute for Advanced Study, Tsinghua University, Beijing 100084, China

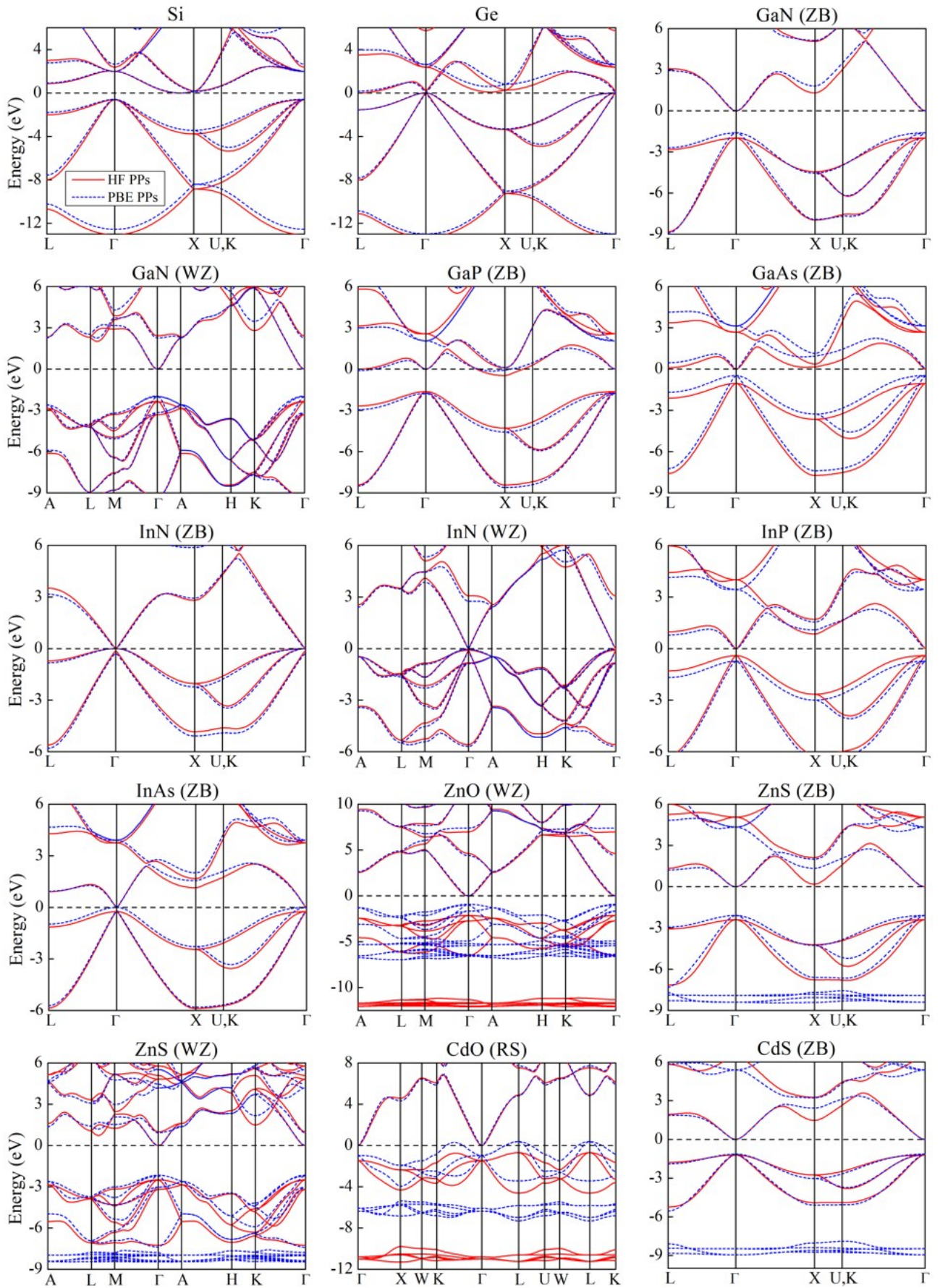*Email: yuancli@bit.edu.cn; zhangs9@rpi.edu; dwh@phys.tsinghua.edu.cn*

Table S1. Parameters for generating the Hartree-Fock pseudopotentials (PP) of the elements considered in the main text. Herein $r_{c,s}$, $r_{c,p}$ and $r_{c,d}$ are the cutoff radii of the s, p and d orbitals, respectively (in atomic unit). Note that we use the same r_c for orbitals with the same angular momentum quantum number for each element.

Atomic number	Symbol	Valence orbitals	$r_{c,s}$	$r_{c,p}$	$r_{c,d}$
7	N	2s2p	1.35	1.54	-
8	O	2s2p	1.34	1.53	-
12	Mg	2s2p3s3p	1.72	1.71	-
14	Si	3s3p	1.70	1.73	-
15	P	3s3p3d4s	1.63	1.63	1.82
16	S	3s3p3d	1.60	1.70	1.88
22	Ti	3p3d4s4p	1.85	1.70	1.80
25	Mn	3p3d4s	1.85	1.78	1.95
30	Zn	3d4s4p	1.87	1.85	1.97
31	Ga	3d4s4p	1.87	2.02	2.01
32	Ge	3d4s4p	1.90	1.90	2.01
33	As	4s4p5s	1.88	1.88	-
34	Se	3d4s4p	2.01	2.02	1.98
48	Cd	4d5s5p	2.00	2.09	1.97
49	In	4d5s5p	1.89	2.03	2.05

Table S2: Band gaps calculated by different PP combinations as well as the experimental values (in eV). The band gap type is either direct (D) or indirect (I). The systems are crystallized in diamond (DM), Zinc-blende (ZB), Wurtzite (WZ), except for MgO and CdO in rocksalt (RS), TiO_2 in rutile (R) and anatase (A), RS MnO in type-II antiferromagnetic configuration, and In_2O_3 in cubic bixbyite.

	System	PP combination				Optimal		Exp.	I/D
		HF+HF	HF+PBE	PBE+HF	PBE+PBE	method	gap		
DM	Si	0.63	-	-	0.59	HF	0.63	1.17[a]	I
	Ge	0.004	-	-	0	HF	0.00	0.74[a]	I
ZB	GaN	1.98	1.93	1.86	1.81	HF+HF	1.98	3.30[b,c]	D
	GaP	1.16	1.57	1.27	1.61	PBE+PBE	1.61	2.35[a]	I
	GaAs	1.04	0.85	0.71	0.51	HF+HF	1.04	1.52[a]	D
	InN	0	0	0	0	-	-	0.78[c]	D
	InP	0.41	0.99	0.14	0.69	HF+PBE	0.99	1.42[a]	D
	InAs	0.24	0.10	0	0	HF+HF	0.24	0.42[a]	D
	ZnO	1.85	1.60	0.93	0.68	HF+HF	1.85	3.27[d]	D
	ZnS	2.40	2.77	1.78	2.10	HF+PBE	2.77	3.72[a]	D
	ZnSe	1.61	1.91	0.99	1.27	HF+PBE	1.91	2.82[a]	D
	CdO (RS)	0.69	0.44	0	0	HF+HF	0.69	0.84[a]	I
	CdS	1.20	1.66	0.74	1.15	HF+PBE	1.66	2.5[e]	D
	CdSe	0.84	1.12	0.36	0.63	HF+PBE	1.12	1.74[a]	D
WZ	GaN	2.35	2.28	2.23	2.16	HF+HF	2.35	3.50[a]	D
	InN	0.10	0.11	0.02	0.02	HF+PBE	0.11	0.78[c]	D
	ZnO	2.13	1.85	1.12	0.86	HF+HF	2.13	3.44[a]	D
	ZnS	2.49	2.84	1.86	2.17	HF+PBE	2.84	3.91[a]	D
	CdS	1.28	1.74	0.81	1.22	HF+PBE	1.74	2.48[a]	D
Other	MgO	5.13	4.80	5.04	4.71	HF+HF	5.13	7.9[a]	D
	TiO_2(R)	1.86	1.83	1.93	1.89	PBE+HF	1.93	3.06[f]	D
	TiO_2(A)	1.97	1.92	2.18	2.14	PBE+HF	2.18	3.20[f]	I
	MnO	1.67	1.62	1.19	0.91	HF+HF	1.67	3.6~4.1[g]	I
	In_2O_3	1.87	1.58	1.43	1.16	HF+HF	1.87	≤2.9[h]	I

[a]Ref.[1], [b]Ref.[2], [c]Ref.[3], [d]Ref.[4], [e]Ref.[5], [f]Ref.[6], [g]Ref.[7], [h]Ref.[8]

Band structure diagrams for Si, Ge, GaN (ZB), GaN (WZ), GaP (ZB), GaAs (ZB), InN (ZB), InN (WZ), InP (ZB), InAs (ZB), ZnO (WZ), ZnS (ZB), ZnS (WZ), CdO (RS), and CdS (ZB). Energy (eV) is plotted versus high-symmetry points. Legend: HF PPs (solid red), PBE PPs (dashed blue).
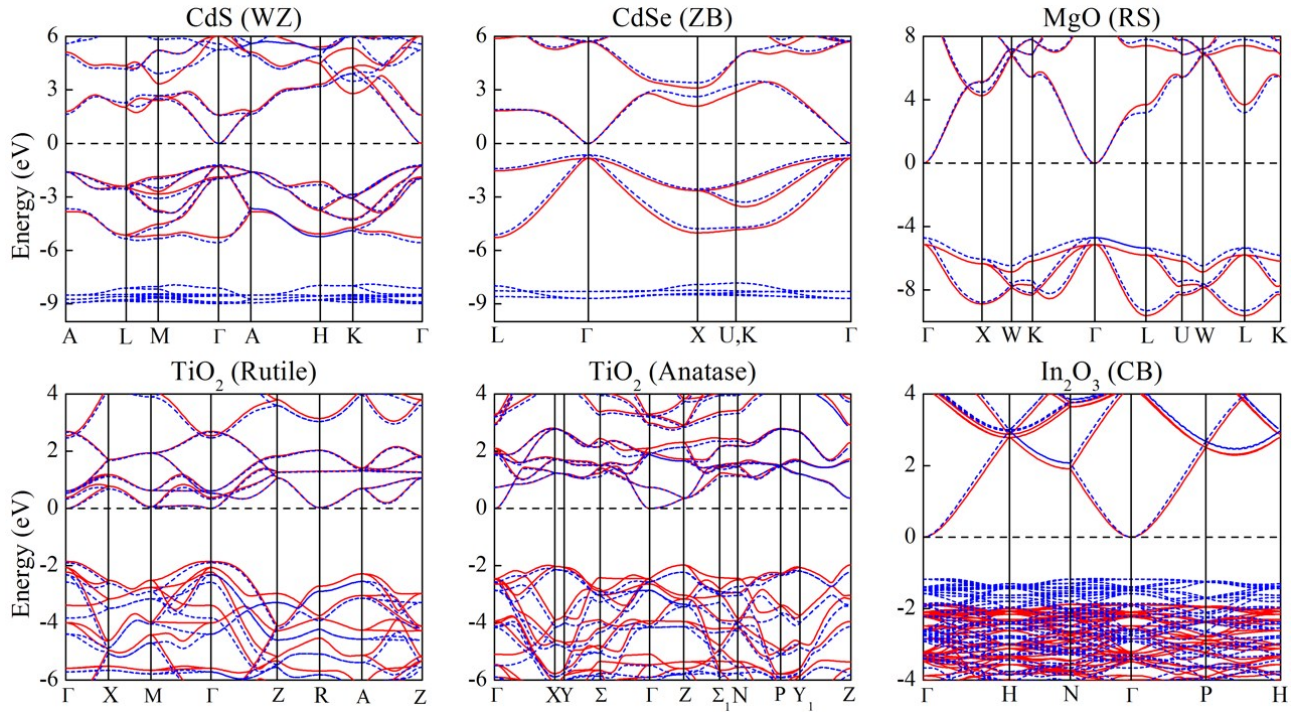
Fig. S1: Band structures of the semiconductors studied in this work. The red solid lines are calculated by employing HF PPs for both cation and anion, while the blue dash lines are calculated by employing PBE PPs for both cation and anion. We take the lowest unoccupied non-d states at the Γ point as the energy reference for binary systems, which is indicated by the horizontal black dashed line in each panel.
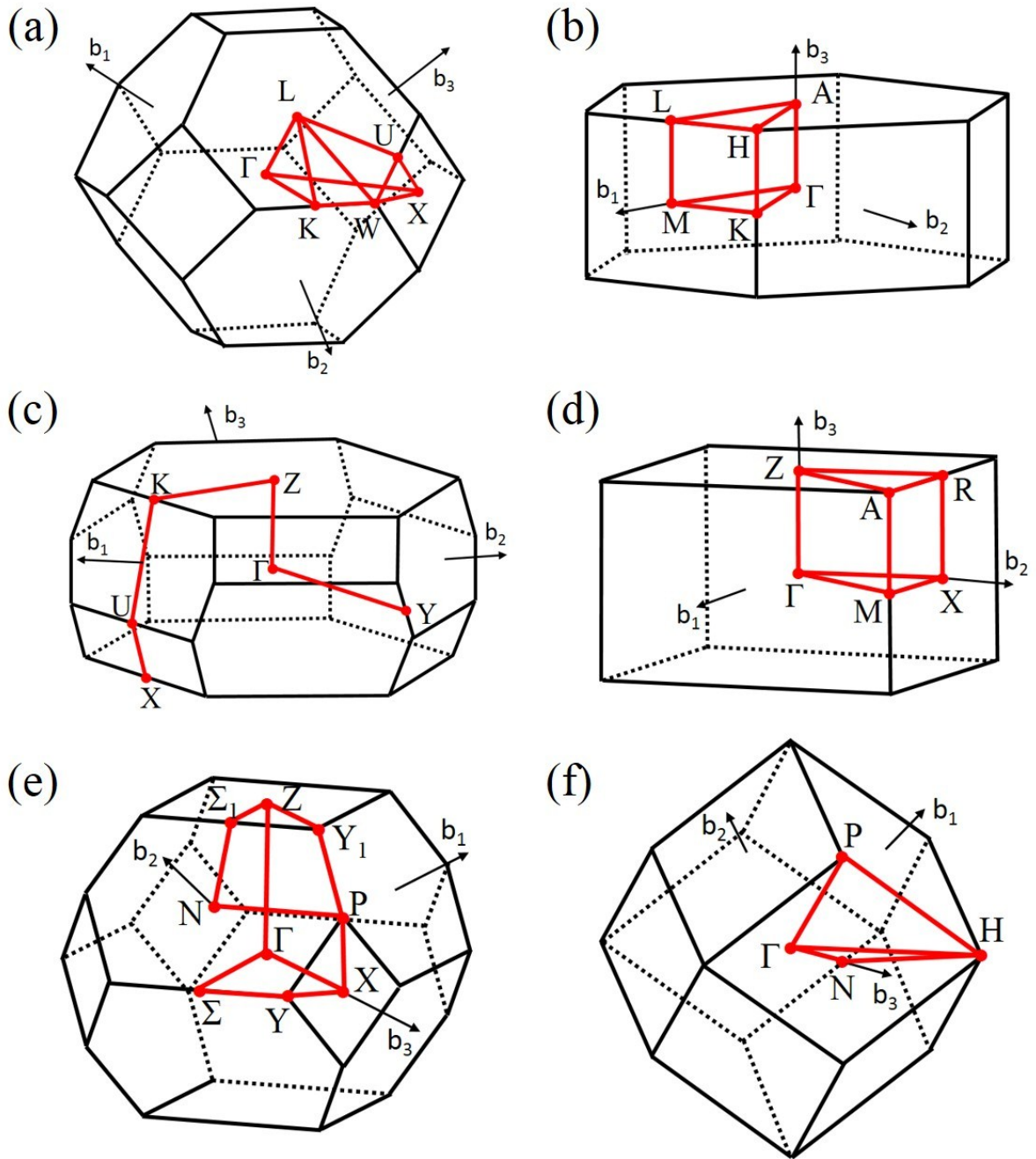
Fig. S2: High symmetry lines in the first Brillouin Zone of (a) diamond, zinc-blende and rocksalt structures, (b) wurtzite structure, (c) MnO (type-II antiferromagnetic rocksalt structure), (d) rutile TiO_2, (e) anatase TiO_2, and (f) cubic bixbyite In_2O_3.
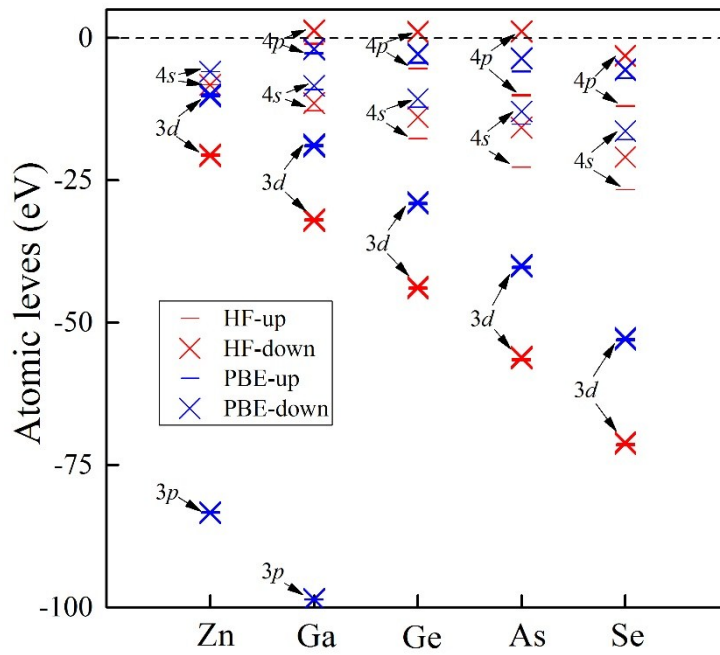
Fig. S3. Atomic levels of Zn, Ga, Ge, As and Se calculated by the all-electron code FHI-aims, respectively within the HF and PBE framework. The "up" and "down" stand for the different spin channels. It shows a general down-shift trend of the (semi)core energy levels by the HF as compared to those by the PBE.
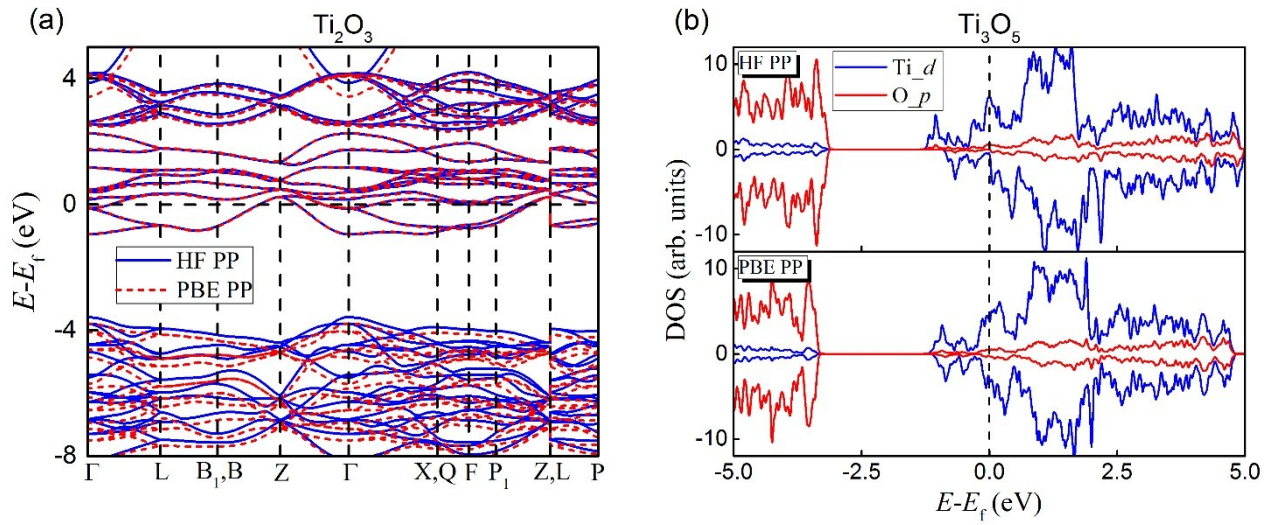
Fig. S4. Electronic structures of (a) Ti_2O_3 (trigonal, space group $R\bar{3}c$) and (b) β-Ti_3O_5 (monoclinic, space group $C2/m$) calculated by the HF and PBE PP, respectively. Due to the low symmetry, we show here only the density of states (DOS) contributed by the Ti d and O p orbitals for the β-Ti_3O_5. Different from the situations of Ti_2O_3 and TiO_2, the Ti_3O_5 is spin-polarized either by the HF or PBE PP calculations. Again, both the HF and PBE PP methods fail to predict a finite band gap for the Ti_2O_3 and β-Ti_3O_5. However, we notice the enhanced spin-polarization by the HF PP in comparison with the PBE PP results. The polarizability at the Fermi level is 86% by the HF PP, much larger than 16% by the PBE PP. Moreover, the former gives local moments of 0.26, 0.07 and 0.12 μ_B at the three Ti atoms while the latter gives 0.08, 0.03 and 0.02 μ_B. These results suggest that the band gap correction by the HF PP on Ti_xO_y compounds is probably limited due to its rather small occupied d-electrons near the Fermi level, but the effect on magnetism might be considerable.

References

[1] O. Madelung, *Semiconductors: Data Handbook* (Springer-Verlag, Berlin Heidelberg, 3rd edition, 2004).

[2] V. Bougrov, M. E. Levinshtein, S. L. Rumyantsev, and A. Zubrilov, *Properties of Advanced Semiconductor Materials GaN, AlN, InN, BN, SiC, SiGe*. Eds. M. E. Levinshtein, S. L. Rumyantsev, M. S. Shur, (John Wiley & Sons, Inc., New York, 2001, 1-30.)

[3] I. Vurgaftman, J. R. Meyer, *J. Appl. Phys.*, 2003, **94**, 3675-3696.

[4] A. B. M. Almamun Ashra, A. Ueta, A. Avramescu, H. Kumano, I. Suemune, Y.-W. Ok, T.-Y. Seong, *Appl. Phys. Lett.*, 2000, **76,** 550-552; S.-K. Kim, S.-Y. Jeong, C.-R. Cho, *Appl. Phys. Lett.*, 2003, **82,** 562-564.

[5] P. E. Lippens, M. Lannoo, *Phys. Rev. B*, 1989, **39**, 10935.

[6] D. Reyes-Coronado, G. Rodríguez-Gattorno, M. E. Espinosa-Pesqueira, C. Cab, R. de Coss, G. Oskam, *Nanotechnology*, 2008, **19**, 145605.

[7] J. van Elp, R. H. Potze, H. Eskes, R. Berger, G. A. Sawatzky, *Phys. Rev. B*, 1991, **44**, 1530; D. R. Huffman, R. L. Wild, M. Shinmei, *J. Chem. Phys.*, 1969, **50**, 4092-4094; R. N. Iskenderov, I. A. Drabkin, L. T. Emelyanova, Y. M. Ksendzov, *Fiz. Tverd. Tela*, 1968, **10**, 2573; E. Z. Kurmaev, R. G. Wilks, A. Moewes, L. D. Finkelstein, S. N. Shamin, J. Kuneš, *Phys. Rev. B*, 2008, **77**, 165127.

[8] R. L. Weiher, R. P. Ley, *J. Appl. Phys.*, 1966, **37**, 299-302; V. Christou, M. Etchells, O. Renault, P. J. Dobson, O. V. Salata, G. Beamson, R. G. Egdell, *J. Appl. Phys.*, 2000, **88**, 5180-5187; P. Erhart, A. Klein, R. G. Egdell, and K. Albe, *Phys. Rev. B*, 2007, **75**, 153205; A. Walsh, J. L. F. Da Silva, S.-H. Wei, C. Korber, A. Klein, L. F. J. Piper, A. DeMasi, K. E. Smith, G. Panaccione, P. Torelli, D. J. Payne, A. Bourlange, R. G. Egdell, *Phys. Rev. Lett.*, 2008, **100**, 167402.